DOR: 20.1001.1.2322388.2020.8.3.5.8

Research Paper

Creep and Stress Redistribution Analysis of Thick-Wall FGM Spheres Subjected to Mechanical Load and Heat Flux – An Analytical Approach

Ali Ziaei-Asl[1*], Mohamadreza Saviz[2], Javad Pourabdollah[3]

1. Assistant Professor, Department of Mechanical Engineering, Azarbaijan Shahid Madani University, Tabriz, Iran
2. Associate Professor, Department of Mechanical Engineering, Azarbaijan Shahid Madani University, Tabriz, Iran
3. Msc Student, Department of Mechanical Engineering, East Azarbaijan Science and Research Branch, Islamic Azad University, Tabriz, Iran.

ARTICLE INFO

Article history:

Received 24 November 2019
Accepted 5 January 2020
Available online 22 July 2020

Keywords:

Creep
Spherical Pressure Vessel
Thermo-mechanical analysis
Functionally Graded Material

ABSTRACT

In this paper, creep analysis of a thick-walled spherical pressure vessel made of Functionally Graded Material (FGM) under thermo-mechanical loadings has been investigated based on Bailey-Norton Law. Considering the nonlinearity of the creep behavior, there is no analytical solution that can accurately determine the stresses of an FGM as a function of time and thermal boundaries, thus in this paper, a new method based on the Taylor Series expansion of the creep strain rate is developed to solve the Beltrami-Michell equation by employing an asymptotic method. The resulting quantities are compared with the numerical ones and show good accuracy. The impacts of FGM constants and wall-thickness, and series order on the creep stress and strain distributions are evaluated. The results are depicted graphically and reveal that even for vessels with high wall thickness and FGM constants, the proposed method equipped with high orders of the Taylor series produces accurate results. Also, due to the agreement of both numerical and analytical methods, this method can be generalized to study the creep of other symmetric FGM structures.

[*] **Corresponding Author:**
Email Address: aziaie@azaruniv.ac.ir

1. Introduction

Conventional composite materials, besides their remarkable advantages such as alteration of properties and orientation of fibers, which might be reformed freely for various goals, suffer from some disadvantages like delamination and failure due to sharp layer-interface [1]. Thus, functionally graded materials, as a new class of composite materials with continuous change of properties in different directions, found a growing application [2]. Multi-functional FGMs are advanced non-homogeneous composites whose structure is microscopically modified to provide desired material properties [3] and is usually made of combining metals and ceramics to increase thermal and mechanical resistance. FGM was first proposed in 1987 by Nino et al. in the Japanese National Aerospace Laboratory to produce a heat-resistant thermal barrier [4], and from then on, it is employed in a variety of applications due to its high versatility [5-7].

Heat exchangers, thermal shields of space structures, reactor walls, engine parts, and all parts exposed to thermo-mechanical stresses such as pressure spherical vessels are some of FGM's industrial applications. Attention should be paid to spherical vessels as they are under long-term thermo-mechanical loadings, which expose the vessel to creep phenomenon. Thus, evaluating the visco-elasto-plastic behavior of FGM vessels is of particular importance [8].

Creep is a complex function of lots of parameters such as stress, time, temperature, material grain size and shape, microstructures, and etc. [9]. Daghigh et al. investigated the initial thermo-elastic and time-dependent creep evolution response of a rotating disk. To achieve the history of stresses, displacements, and creep strains, a numerical procedure using Taylor series and Prandtl-Reuss relation is utilized, which offers radial, circumferential and effective stress and strain histories [10]. To experimentally study the creep phenomenon, a series of uniaxial creep tests has been conducted by Cen and et al. [11] at 650° C. The experimental data have been applied to the structural integrity assessment of a thin-walled pressure vessel. Pathania and Verma [12] studied the temperature and pressure-dependent creep stress analysis of a spherical shell. Evaluating the effect of different parameters indicated that parameter n has a significant influence on the creep stresses and strain rates.

Several researchers have studied the creep and thermo-elastic behavior of thick-walled vessels made of FGMs in the literature. A general analytical solution for one-dimensional steady-state thermal and mechanical stresses in an FG hollow sphere is done by Eslami et al. [13]. Bayat et al. [14] presented an analytical and numerical solution to obtain symmetric thermal and mechanical stresses in a thick-walled FG sphere under pressure and thermal loadings. Stresses and strains on an FGM cylinder under mechanical and thermal loading has been theoretically derived by Habib [15]. The results have been compared with the stresses obtained from a finite element simulation. Loghman et al. [16] investigated time-dependent creep stress redistribution of a thick-walled FGM sphere subjected to internal pressure and uniform temperature using successive elastic solution method. Jafari Fesharki et al. [17] used a semi-analytical numerical method as well as Prandtl-Reuss and Sherby relations to analyze the time-dependent creep behavior of an FG hollow sphere under thermomechanical loading. Yang [18] analyzed the time-dependent FGM cylindrical vessel considering the creep behavior of the structure. Based on the results obtained, the higher-order solution can be used to calculate the stresses for a long time creeping. In the presence of time-dependent heat resource, the heat conduction equation is numerically solved for a two-dimensional hollow FG cylinder by Daneshjou et al. [19]. Delouei and et al. [20] obtained an analytical solution for the two-dimensional steady-state heat transfer with general thermal boundary conditions in an FGM hollow sphere.

Considering the extensive research on the thermo-mechanical behavior of materials in the recent decade, the literature is quite narrow in FGM pressure vessels, especially the studies using analytical solutions. Furthermore, considering the creep behavior of FGMs, there are no analytical solutions that can accurately determine the stresses as a function of time and thermal boundaries conditions; and others are often examined the problem by conventional approximation and numerical methods. In this paper, the creep behavior of an FGM spherical vessel subjected to a uniform thermal flux and mechanical load is investigated by a new analytical procedure based on the asymptotic method. The effects of different parameters on the stress and strain fields are studied. Moreover, to validate the results of proposed method, a finite element analysis has been conducted.The results derived from the equations are compared with the numerical results from the simulation.

2. Problem Formulation and Method

2.1 Mathematical Approach

A thick-walled spherical vessel made of functionally graded material is of concern. The inner and outer radii are *a* and *b*, respectively. The vessel is subjected to uniform internal and external pressure P_i and P_o,

respectively. The interior surface is exposed to a thermal flux, while the exterior surface experiences a convective heat transfer with the environment. In this paper, it is assumed that the material of the FG pressure vessel is graded according to a power law in the following forms [21]:

$$K_{(r)} = K_i \left(\frac{r}{a}\right)^{\beta_1}$$
$$E_{(r)} = E_i \left(\frac{r}{a}\right)^{\beta_2} \quad (1)$$
$$\alpha_{(r)} = \alpha_i \left(\frac{r}{a}\right)^{\beta_3}$$

where K_i, E_i , and α_i are respectively thermal conductivity, elasticity modulus, and coefficient of thermal expansion at the inner surface of the vessel. β_1 , β_2 and β_3 are the graded factor of the FGM vessel. The Poisson's ratio is assumed as constant.

2.2 Conductive Heat Transfer Analysis

Due to spherical symmetry in the geometry, as well as loading and boundary conditions, the system of governing equations of heat is as follows:

$$\frac{1}{r^2}\frac{d}{dr}\left(K_{(r)} r^2 \frac{dT}{dr}\right) = 0 \quad (2)$$

The boundary conditions of the internal and external surfaces of the vessel are:

$$\begin{cases} -K_i \left.\dfrac{dT}{dr}\right|_{r=a} = q \\ hT\,\Big|_{r=b} + K_0 \left.\dfrac{dT}{dr}\right|_{r=b} = hT_\infty \end{cases} \quad (3)$$

where T_∞ is the ambient temperature, and h is the convective heat transfer coefficient. By embedding the thermal conductivity of FGM in the heat equation:

$$T_{(r)} = c_1 r^{-1-\beta_1} + c_2 \quad (4)$$

where c_1 and c_2 will be found from boundary conditions as:

$$\begin{cases} c_1 = \dfrac{q a^{\beta_1+2}}{K_i(1+\beta_1)} \\ c_2 = T_\infty + \left(\dfrac{K_0}{K_i}\right)\left(\dfrac{a}{b}\right)^{\beta_1+2}\left(\dfrac{q}{h}\right) + \left(\dfrac{a}{b}\right)^{\beta_1+1}\left(\dfrac{aq}{K_i(1+\beta_1)}\right) \end{cases} \quad (5)$$

3. Analytical Solution

Various creep model equations are in use to represent the time-dependent deformation of the engineering materials [22]. In this study, Baily-Norton creep equation is used to describe creep behavior [23].

$$\varepsilon_{eq}^c = B\sigma_{eq}^N t^x \quad (6)$$

where B is the creep strain hardening coefficient. B, N, and x are temperature-dependent material constants that are generally independent of stress and are derived from uniaxial creep tests. Assuming x equal to 1, the Norton law models the secondary stage or steady-state section of creep phenomenon, in which strain rate is constant. Steady-state creep occurs after time-dependent strain rate stage, called transient or primary creep, when after a long period of time, the stress reaches a constant value over time. Stresses, strains, and displacements in a structure are determined using elasticity theory. By considering strain-displacement relations, Hooke's structural relation, and the static equilibrium equation in one element of the structure, this theory forms the system of differential equations that can be in terms of stress, strain, or displacement. In addition to the mechanical strains, thermal strains caused by the temperature gradient in the structure, should be considered in Hooke's structural equation, which establishes thermo-elastic formulation of the structure.

Due to the spherical symmetry, the circumferential components, θ and φ, of the stress and strains will be equal. In this case, the equilibrium equation, strain compatibility equation, and Hook's general law in terms of strain components, which are a combination of elastic, thermal, and creep strains, are as follows:

$$\frac{d\sigma_{rr}}{dr} + \frac{2}{r}(\sigma_{rr} - \sigma_{\theta\theta}) = 0 \quad (7)$$

$$\frac{d\mathcal{E}_{\theta\theta}}{dr} + \frac{(\mathcal{E}_{\theta\theta} - \mathcal{E}_{rr})}{r} = 0 \quad (8)$$

$$\mathcal{E}_{rr} = \frac{1}{E}[\sigma_{rr} - 2\vartheta\sigma_{\theta\theta}] + \alpha\big(T(\mathrm{r,t}) - T_{ref}\big) + \mathcal{E}_{rr}^c \quad (9)$$

$$\mathcal{E}_{\theta\theta} = \frac{1}{E}[(1\text{-}\vartheta)\sigma_{\theta\theta} - \vartheta\sigma_{rr}] + \alpha(T(\mathrm{r,t}) - T_{ref}) + \mathcal{E}_{\theta\theta}^c \quad (10)$$

By embedding these equations and performing some simplifications, the Beltrami-Michell differential equation will be obtained in terms of radial stress of the vessel:

$$\begin{aligned} r^2\frac{d^2\sigma_{rr}}{dr^2} + r(4-\beta_2)\frac{d\sigma_{rr}}{dr} - 2\beta_2\left(\frac{1-2\vartheta}{1-\vartheta}\right)\sigma_{rr} \\ = -\frac{2\alpha_i E_i\, r^{\beta_2+\beta_3+1}}{(1-\vartheta)a^{\beta_2+\beta_3}}\frac{dT}{dr} - \frac{2\alpha_i E_i \beta_3\, r^{\beta_2+\beta_3}}{(1-\vartheta)a^{\beta_2+\beta_3}}T \\ - \frac{2E_i\, r^{\beta_2+1}}{(1\text{-}\vartheta)\, a^{\beta_2}}\frac{d\mathcal{E}_{\theta\theta}^c}{dr} \\ - \frac{2E_i\, r^{\beta_2}}{(1\text{-}\vartheta)\, a^{\beta_2}}(\mathcal{E}_{\theta\theta}^c - \mathcal{E}_{rr}^c) \end{aligned} \quad (11)$$

To solve this equation, it is necessary to transform the complex and nonlinear governing equation of strain rate, into simple polynomials. For this purpose, a method based on the Taylor series expansion for the components of creep strain rate is employed. Creep strains are zero in terms of the elastic solution, but at subsequent time steps, they will be obtained by the following equation:

$$\mathcal{E}^{\,c}_{(j+1)} = \mathcal{E}^{\,c}_{(j)} + \dot{\mathcal{E}}^{\,c}_{(j)}\Delta t \tag{12}$$

Using the creep equation, the rates of the components of the creep strain at each *j*th time stepstage are found to be:

$$\dot{\mathcal{E}}^{c}_{rr} = \frac{3}{2}B\sigma_{eq}^{(N-1)}S_{rr} \tag{13}$$

$$\dot{\mathcal{E}}^{c}_{\theta\theta} = \frac{3}{2}B\sigma_{eq}^{(N-1)}S_{\theta\theta} \tag{14}$$

The values of σ_{eq} and S_{rr} and $S_{\theta\theta}$ are as:

$$\sigma_{eq} = |\sigma_{rr} - \sigma_{\theta\theta}| \tag{15}$$

$$S_{rr} = \frac{2}{3}(\sigma_{rr} - \sigma_{\theta\theta}) \tag{16}$$

$$S_{\theta\theta} = \frac{1}{3}(\sigma_{\theta\theta} - \sigma_{rr}) \tag{17}$$

In these equations, σ_{eq}, S_{rr}, and $S_{\theta\theta}$, are respectively the equivalent stress, radial deviator stress, and circumferential deviator stress of the vessel at each time step.

At *time=0*, the stress components are obtained by the solution of the differential equation. At the following time steps, by calculating the creep strain rate at each time interval, the value of creep strain at each moment is obtained. Then, total strain and stress at the next time step will be found. Therefore, at each time step, the creep strain rate can be expressed in terms of stress components as:

$$\dot{\mathcal{E}}^{c}_{rr}\Big|_{t_j} = B|\sigma_r - \sigma_\theta|^{N-1}.(\sigma_r - \sigma_\theta)|_{t_j} \tag{18}$$

$$\dot{\mathcal{E}}^{c}_{\theta\theta}\Big|_{t_j} = -\frac{B}{2}|\sigma_r - \sigma_\theta|^{N-1}.(\sigma_r - \sigma_\theta)|_{t_j} \tag{19}$$

Knowing that the volume does not change in a plastic flow, it can be concluded that the sum of the creep strain rates should be zero:

$$\dot{\mathcal{E}}^{c}_{\theta\theta}\Big|_{t_j} = -\frac{1}{2}\dot{\mathcal{E}}^{c}_{rr}\Big|_{t_j} \tag{20}$$

Taylor series expansion of the creep strain rate is:

$$\dot{\mathcal{E}}^{c}_{rr}\Big|_{t_j} = \sum_{k=0}^{k=n} A_k^{(j)}(r-\bar{r})^k \tag{21}$$

where;

$$A_k^{(j)} = \frac{1}{k!}\left[\frac{d^k}{dr^k}(\dot{\mathcal{E}}^{c}_{rr}\Big|_{t_j})\right]_{r=\bar{r}}^{0} \tag{22}$$

The parameter *j* is time step counter, *n* is the Taylor series order, *k* is the derivative order, and $\bar{r}$ is the coordinate of the vessel wall's midpoint.

Substituting temperature and creep strain equations into the Beltrami-Michell equation, the governing differential equation at the *j*th time step will be found as:

$$r^2\frac{d^2\sigma_{rr}^{(j)}}{dr^2} + r(4-\beta_2)\frac{d\sigma_{rr}^{(j)}}{dr} - 2\beta_2\left(\frac{1-2\vartheta}{1-\vartheta}\right)\sigma_{rr}^{(j)} = c_3 r^{\beta_3+\beta_2-\beta_1-1} + c_4 r^{\beta_3+\beta_2} + \sum_{k=0}^{k=m} I_k^{(j)} r^{k+\beta_2} \tag{23}$$

where;

$$c_3 = \frac{2E_i\alpha_i(1+\beta_1-\beta_3)}{(1-\vartheta)(a^{\beta_2+\beta_3})}.c_1 \tag{24}$$

$$c_4 = \frac{-2E_i\alpha_i\beta_3}{(1-\vartheta)(a^{\beta_2+\beta_3})}.c_2 \tag{25}$$

$$I_k^{(j)} = \frac{2E_i[X_k^{(j)} - (k+1)Y_k^{(j)}]}{(1-\vartheta)\,a^{\beta_2}} \tag{26}$$

The solution of this differential equation, which is a Cauchy-Euler type, is given by:

$$\sigma_{rr}^{(j)} = d_1^{(j)}r^{\xi_1} + d_2^{(j)}r^{\xi_2} + d_3^{(j)}r^{\xi_3} + d_4^{(j)}r^{\xi_4} + \sum_{k=0}^{k=m} H_k^{(j)}r^{k+\beta_2} \tag{27}$$

where the coefficients are as:

$$\xi_1 = \left(\frac{\beta_2-3}{2}\right) + \sqrt{\left(\frac{\beta_2-3}{2}\right)^2 + 2\beta_2\left(\frac{1-2\vartheta}{1-\vartheta}\right)} \tag{28}$$

$$\xi_2 = \left(\frac{\beta_2-3}{2}\right) + \sqrt{\left(\frac{\beta_2-3}{2}\right)^2 + 2\beta_2\left(\frac{1-2\vartheta}{1-\vartheta}\right)} \tag{29}$$

$$\xi_3 = \beta_3 + \beta_2 - \beta_1 - 1 \tag{30}$$

$$\xi_4 = \beta_3 + \beta_2 \tag{31}$$

$$d_3 = \frac{c_3}{\xi_3^2 + (3-\beta_2)\xi_3 - 2\beta_2\left(\frac{1-2\vartheta}{1-\vartheta}\right)} \tag{32}$$

$$d_4 = \frac{c_4}{\xi_4^2 + (3-\beta_2)\xi_4 - 2\beta_2\left(\frac{1-2\vartheta}{1-\vartheta}\right)} \tag{33}$$

$$H_k^{(j)} = \frac{I_k^{(j)}}{(k+\beta_2)^2 + (3-\beta_2)(k+\beta_2) - 2\beta_2\left(\frac{1-2\vartheta}{1-\vartheta}\right)} \tag{34}$$

The parameters $d_{1(j)}$ and $d_{2(j)}$ are the constants of integration and can be calculated from the boundary conditions. Finally, at each time step, the radial stress is obtained as:

$$\sigma_{rr} = \sum_{k=1}^{k=4} d_k r^{\xi_k} + \sum_{k=0}^{k=m} H_k r^{k+\beta_2} \tag{35}$$

Substituting the radial stress into the equilibrium equation, circumferential stress will be obtained as:

$$\sigma_{\theta\theta} = \sum_{k=1}^{k=4} d_k \left(1+\frac{\xi_k}{2}\right) r^{\xi_k} + \sum_{k=0}^{k=m} H_k \left(1+\frac{k+\beta_2}{2}\right) r^{k+\beta_2} \quad (36)$$

Therefore, the distribution of the equivalent stress in the wall-thickness of the FGM sphere will be determined by:

$$\sigma_{eq} = \left| \sum_{k=1}^{k=4} \frac{1}{2}\xi_k d_k r^{\xi_k} + \sum_{k=0}^{k=m} \frac{1}{2}(k+\beta) H_k r^{k+\beta_2} \right| \quad (37)$$

Total strains at each time-step can be found by substituting the above stress equations and creep strains as well as temperature distribution equation (4) into equations (9) and (10).

$$\mathcal{E}_{rr} = \sum_{k=1}^{k=4} d_k^* r^{\xi_k-\beta_2} + \sum_{k=0}^{k=m} (H_k^*+X_k) r^k + c_1^* r^{\beta_3-\beta_1-1} + c_2^* r^{\beta_3} \quad (38)$$

$$\mathcal{E}_{\theta\theta} = \sum_{k=1}^{k=4} d_k^{**} r^{\xi_k-\beta_2} + \sum_{k=0}^{k=m} (H_k^{**}+Y_k) r^k + c_1^* r^{\beta_3-\beta_1-1} + c_2^* r^{\beta_3} \quad (39)$$

where:

$$d_k^* = \frac{a^{\beta_2}}{E_i}\left[1-2\vartheta\left(1+\frac{\xi_k}{2}\right)\right] d_k \quad (40)$$

$$H_k^* = \frac{a^{\beta_2}}{E_i}\left[1-2\vartheta\left(1+\frac{k+\beta_2}{2}\right)\right] H_k \quad (41)$$

$$d_k^{**} = \frac{a^{\beta_2}}{E_i}\left[(1-\vartheta)\left(1+\frac{\xi_k}{2}\right)-\vartheta\right] d_k \quad (42)$$

$$H_k^{**} = \frac{a^{\beta_2}}{E_i}\left[(1-\vartheta)\left(1+\frac{k+\beta_2}{2}\right)-\vartheta\right] H_k \quad (43)$$

$$c_1^* = a^{-\beta_3}\alpha_i c_1 \quad (44)$$

$$c_2^* = a^{-\beta_3}\alpha_i c_2 \quad (45)$$

Using the strain-displacement equation, we can also provide a radial displacement distribution at each time step as:

$$u_r = \sum_{k=1}^{k=4} d_k^{**} r^{\xi_k-\beta_2+1} + \sum_{k=0}^{k=m} (H_k^{**}+Y_k) r^{k+1} + c_1^* r^{\beta_3-\beta_1} + c_2^* r^{\beta_3+1} \quad (46)$$

4. Numerical Modeling

For a comparative study, a finite element numerical model of the FGM vessel was developed in order to verify the results of the proposed formulation. Due to symmetry, only a quarter of the vessel was modeled. The model has been developed as an axisymmetric shell, and the spherical coordination system is used. In order to execute non-homogeneous behavior of the vessel's thickness, the wall is discretized into numerous ultra-thin layers along the radial direction, and the material properties for each layer are obtained by using Eq. (1).

A Mesh sensitivity study has been conducted to find the appropriate element size, therefore,9664 of 8-node axisymmetric thermally coupled quadrilateral, biquadratic displacement, bilinear temperature, reduced integration elements, and 26125 nodes are employed to analyze the thermal and mechanical field of the model.

The thermal and mechanical loadings were applied as boundary conditions. To model the creep behavior, a power-law model utilized by active strain-hardening, along with two coupled thermal-displacement analyses, one for the steady-state elastic solution, and the other one for the creep solution, have been applied. The model is solved to compute the strain and stress fields during and after creep up to 55000 seconds in each condition.

5. Results and Discussion

In the following section, a FE numerical model is used to validate the results of the analytical solution. Furthermore, the influence of different parameters on the accuracy and efficiency of the proposed method has been investigated. These parameters include the thickness of the vessel, the gradient properties of FGM in the radial direction, and the Taylor series order.

5.1 Analytical Method Validation

For verifying the proposed method, the analytical solution and numerical analysis presented in the previous sections were applied to a thick FGM spherical pressure vessel with inner and outer radii, respectively equal to $a = 20\ mm$ and $b = 40\ mm$, as a case study. The data in Table 1 are implemented in the analysis. Mechanical and thermal properties of the material are assumed to obey the power-law variation with $\beta_i=0.1$, and the Taylor series of order 9 is adopted to calculate the stress and strain fields. Stress and strain distributions, as well as deformations and temperature in the FGM spherical vessel at *time=0* (equivalent to thermo-elastic solution) and during stress rearrangement and creep period, have been evaluated.

Table 1. Loading and material properties of the FGM sphere used in the case study [21]

Property	Unit	Value
P_i	MPa	80
P_o	MPa	0
E_i	GPa	207
α_i	k^{-1}	10.8×10^{-6}
K_i	w/m°C	43
ν	-	0.292
q	w/m^2	3000
h	$W/m^2°C$	6.5
$T\infty$	°C	25
N	-	2.25
B	-	1.4×10^{-8}

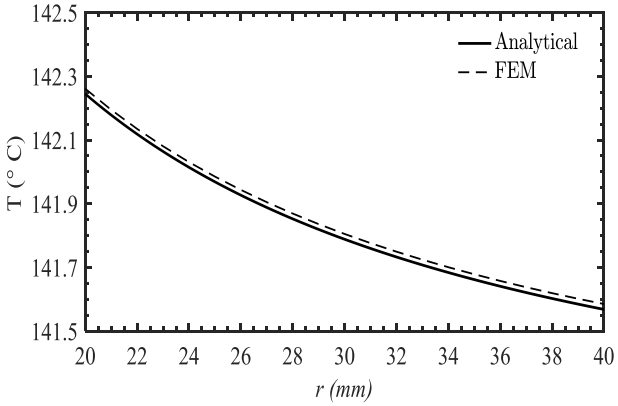

Fig. 1. Temperature distribution along the thickness of FGM spherical

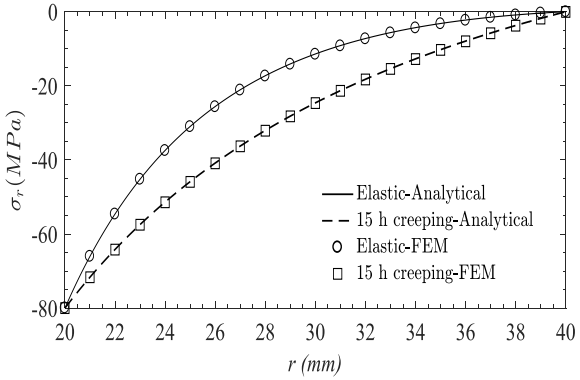

a) radial stress

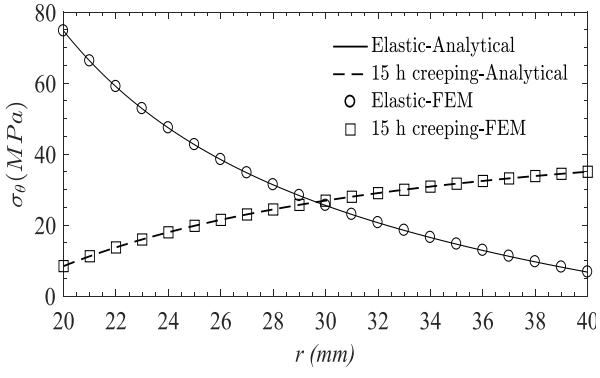

b) circumferential stress

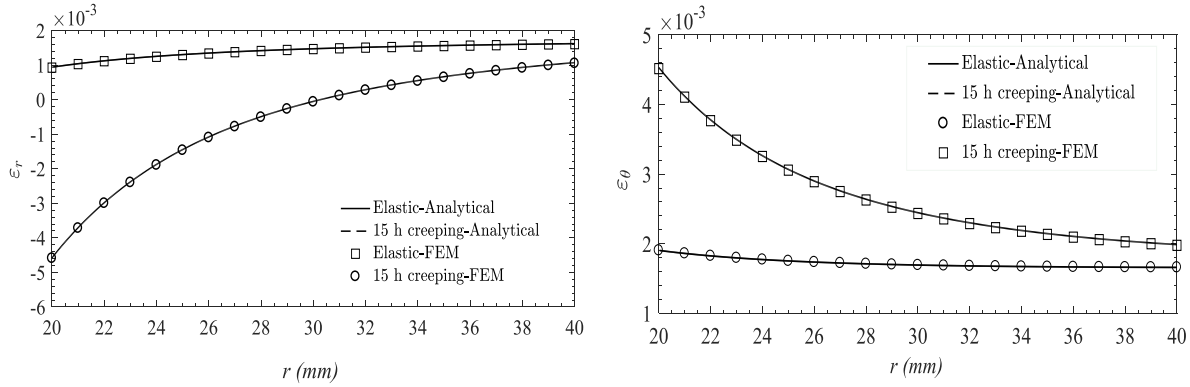

c) radial strain d) circumferential strain

Fig. 2. Stress and strain distributions of FGM sphere in elastic mode and after 15-hour creep calculated by numerical and analytical methods

Fig. 2 shows the distribution of temperature through the wall thickness of the FGM sphere. A comparison between the results indicates that the analytical solution has good accuracy. The distributions of radial and circumferential stresses and strains for the thermo-elastic stage and 15-hour creep, resulting from numerical and analytical methods, are plotted in Fig. 2. As shown in Fig. 2a, the gradient of the radial stress along the wall-thickness, r, reduces over time due to the creeping behavior of the FGM sphere. Except for the boundary points, after 15 hours of creeping, the radial stress reaches a relaxation level, which is called stress rearrangement. This phenomenon occurs for circumferential stress either. As depicted in Fig. 2c, it can be seen that while the radial strain of the thickness is tensile at the elastic stage, it decreases to compressive values after creeping, especially on the inner surface, which indicates that the inner surface of the sphere encounters a high compression, and the wall becomes thinner. On the contrary, the circumferential strain through the wall is tensile and increases over time (Fig. 2d). Consequently, it can be stated that the inner surface experiences high radial and circumferential strains.

Fig. 3 illustrates radial displacement at a time equal to zero and after 15-hour creep, calculated by numerical and analytical methods. It shows that after 15 hours, the radial displacement of the wall increases up to 3 times.

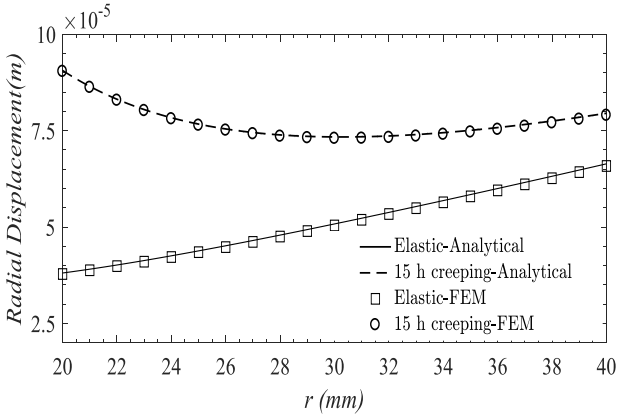

Fig. 3. Radial displacement distribution of FGM sphere in elastic mode and after 15 hours of creeping calculated by numerical and analytical method

For a better understanding of the stress rearrangement, strain and stress histories of three layers of the vessel's thick wall with equal distances are studied. Fig. 4 displays the variations of radial and circumferential stresses and strains in these layers. As can be seen from Fig. 4c-d, strain variations at inner layers are more severe. Moreover, whereas radial strain changes to compressive strain over time, the circumferential strain becomes more extensional. Fig. 4a-b shows that the stress components vary over time only at the first hours. Afterward, stress components almost remain unchanged, while creep strain rises continuously, up to a rupture, predictably at the points where the growth rate of creep strain is higher. On the other hand, one can deduce that by progressing creep strains, tensile stress moves from the high-stresses points to the points with lower strain rates.

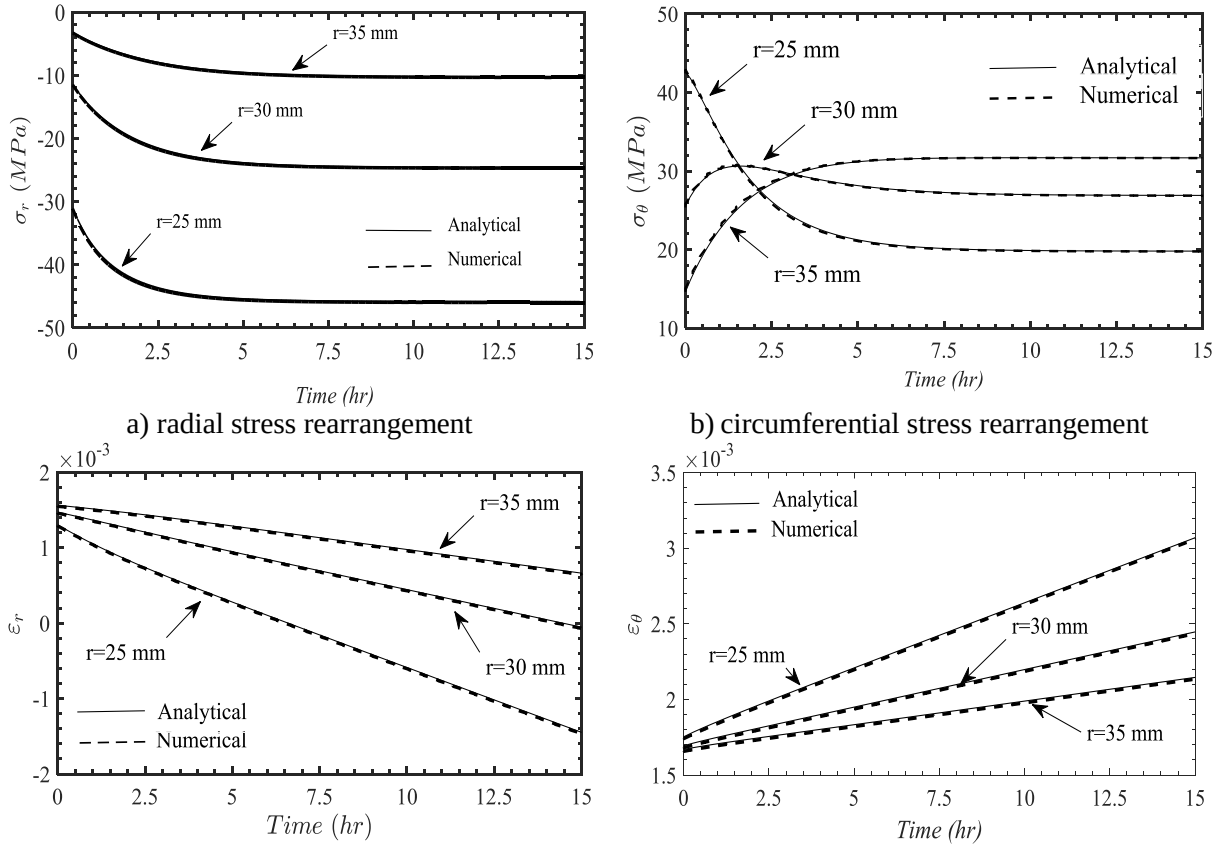

a) radial stress rearrangement b) circumferential stress rearrangement

c) radial strain d) circumferential strain

Fig. 4. variations of stresses and strains at three layers of sphere-wall

In this section, the creep behavior of the vessel has been investigated by using the proposed method based on the Taylor series as well as the finite element method. Comparing the results from the two methods showed that the results obtained from the proposed method, including temperature, stress, strain, and displacement, are in good agreement with the ones from FEM.

5.2 Influence of the Effective Factors on the Accuracy of the Proposed Method

In this section, the order of Taylor Series for strain-rate approximation, distribution of FGM properties, and wall thickness of the vessels have been chosen as parameters affecting the accuracy of the method.

The Effect of Taylor Series order

Here, to investigate the effect of Taylor series order on the accuracy of the proposed method, different orders of Taylor series are adopted, while the other conditions are the same as. The results have been compared with finite element results. The distribution of circumferential stresses after stress rearrangement is shown in Fig. 5 for the series orders of 3, 5, and 7.

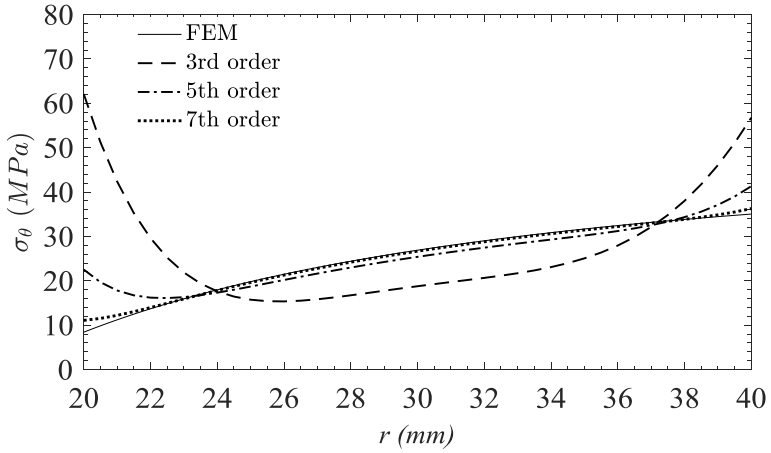

Fig. 5. Steady-state circumferential stress distribution computed by FEM and different orders of Taylor series

It can be found out that the major computational errors occur at the inner and outer surfaces of the sphere, which can be minimized by increasing the series order. Fig. 6 displays the histories of equivalent stress at the inner and middle layers of the wall with different Taylor orders. It shows that using low orders of the series leads to divergence of the results and, by using higher orders of the Taylor series, the responses converge. Therefore, it is essential to select the appropriate order of the series to obtain accurate results.

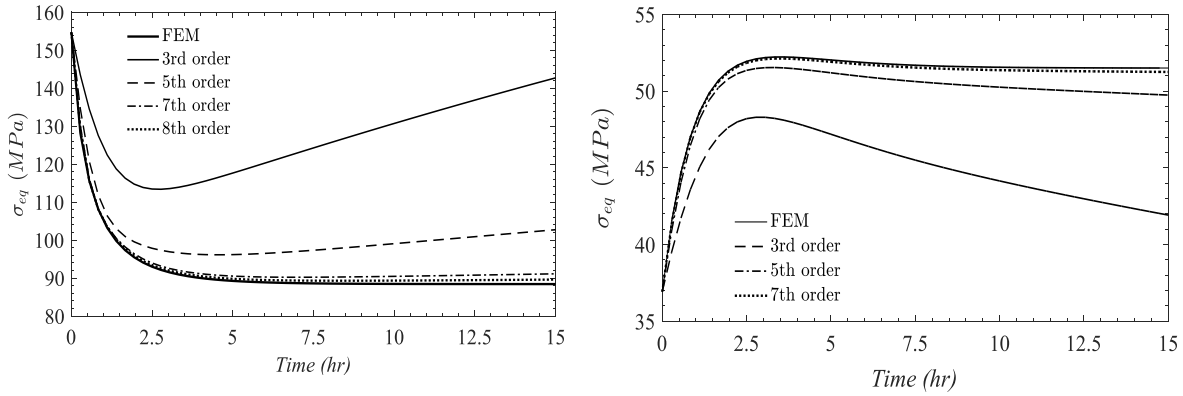

a) equivalent stress rearrangement at r=20mm b) equivalent stress rearrangement at r=30mm

Fig. 6. Variations of equivalent stress at the inner and middle surfaces of FGM spherical with different orders of Taylor series

The Effect of the Distribution of FGM Physical Properties

In order to study the effect of the FGM properties on the accuracy of the proposed method, the case study sphere with varying values of β (= -0.1, -0.9, -2, -3) has been analyzed. Fig. 7 plots the variation of steady circumferential stress through the wall-thickness for β = -0.9, -2. One can deduce that β constant does not affect the steady-state stress distribution during creep; meanwhile, more accurate responses are obtained with higher orders of the Taylor series. Furthermore, it can be seen that the inner surface is the most sensitive point to series order. For varying values of β and different orders of Taylor series, a detailed comparison about the steady circumferential stress at the inner surface of the sphere, computed by FEM and proposed method, is presented in Table 2.

Table 2. Steady circumferential stress values and error percentage at the inner surface of the FGM sphere, for different values of β and Taylor Series order

		β (grade factor of the FGM)				
Series Order		-0.1	-0.3	-0.9	-2	-3
5	σ_θ (MPa)	22.06	25.56	28.32	44.46	64.66
	Error (%)	162	203.56	236.34	428.03	667.93
6	σ_θ (MPa)	14.94	16.57	17.67	24.85	33.49
	Error (%)	77.43	96.79	109.86	195.13	297.74
7	σ_θ (MPa)	10.99	11.66	12.17	15.20	19.29
	Error (%)	30.52	38.48	44.54	80.52	129.10
8	σ_θ (MPa)	9.54	9.83	10.01	11.21	12.14
	Error (%)	13.30	16.75	18.88	33.14	44.18
9	σ_θ (MPa)	8.85	8.97	9.04	9.58	10.70
	Error (%)	5.11	6.53	7.36	13.78	27.91
10	σ_θ (MPa)	8.61	8.65	8.71	8.96	9.32
	Error (%)	2.26	2.73	3.44	6.41	10.69
FEM	σ_θ (MPa)			8.42		

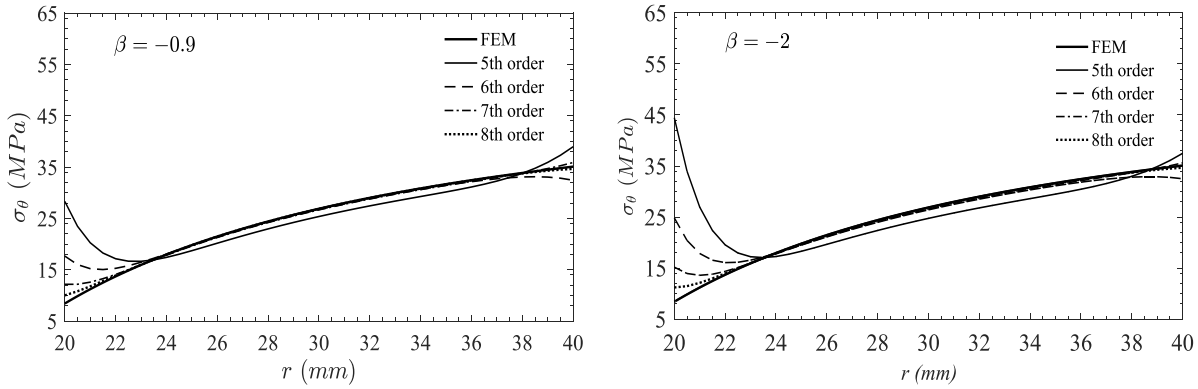

a) circumferential stress for β= - 0.9 b) circumferential stress for β=-2

Fig. 7. Distribution of steady circumferential stress in FGM sphere wall for two different β constants

Considering the error, it can be concluded that for a specific order of the Taylor series, the smaller value of β, the more accurate results will be. Therefore, for FGMs with high-intensity gradients, higher Taylor orders should be used.

The Effect of the Vessel Geometry

Another key parameter is the thickness of the vessel. Fig. 8 shows the influence of the wall thickness on the distribution of steady circumferential stress of the wall. It can be seen that at the inner and outer surfaces, stress values are more sensitive to the Taylor series order.

The results show that with the increase in the sphere wall thickness, it is necessary to use high orders of Taylor series to obtain acceptable solutions.

Table 3 presents the value of steady circumferential stress on the sphere's inner surface for different wall thicknesses and Taylor series orders. According to this table, while the lower orders lead to acceptable results in the thinner sphere walls, for the thick-wall spheres, higher orders should be employed.

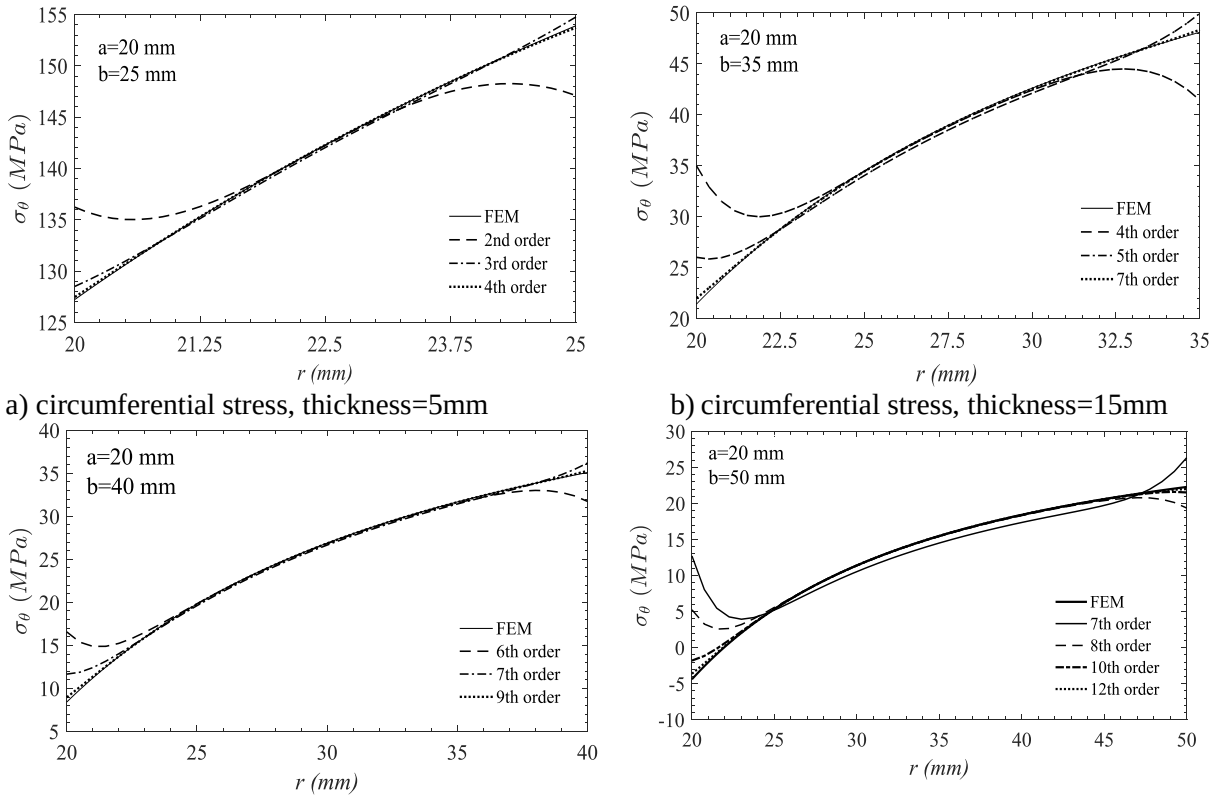

a) circumferential stress, thickness=5mm b) circumferential stress, thickness=15mm

c) circumferential stress, thickness=20mm d) circumferential stress, thickness=30mm

Fig. 8. Distribution of steady circumferential stress through FGM sphere wall with varying thickness

Table 3. Steady circumferential stress at the inner surface of the FGM sphere with different wall thicknesses

		Wall Thickness (mm)			
Series Order		5	10	15	20
3	σ_θ (MPa)	128.5	51.55	50.56	72.20
	Error (%)	1.02	8.05	135.93	757.48
4	σ_θ (MPa)	127.5	48.94	34.99	48.47
	Error (%)	0.24	2.58	63.28	475.65
5	σ_θ (MPa)	127.28	47.96	26.01	25.56
	Error (%)	0.06	0.52	21.37	203.56
6	σ_θ (MPa)	---	47.74	23.19	16.57
	Error (%)	---	0.06	8.21	96.79
7	σ_θ (MPa)	---	---	22.00	11.66
	Error (%)	---	---	2.66	38.48
8	σ_θ (MPa)	---	---	21.63	9.83
	Error (%)	---	---	0.93	16.75
9	σ_θ (MPa)	---	---	---	8.97
	Error (%)	---	---	---	6.53
10	σ_θ (MPa)	---	---	---	8.65
	Error (%)	---	---	---	2.73
FEM	σ_θ (MPa)	127.2	47.71	21.43	8.42

6. Conclusion

In this paper, an analytical method based on the Taylor series is introduced to study the creep behavior of an FGM thick-walled sphere under mechanical and thermal loadings with the Baily-Norton model. To achieve the steady-state solution, the asymptotic method is employed, and the histories of strain and stress are presented at the initial elastic stage and then at steady-state creep stage. The results have been compared with the results of a developed FE model, and good agreements have been observed. The effects of FGM material constants, wall-thickness of the sphere, and order of the series on the accuracy of the proposed method have been studied and discussed in detail.

By investigating temperature, stress and strain fields, it is concluded that the order of Taylor series has a significant influence on strains and stresses of the vessel, and the following results are obtained:

- The analytical method can solve the heat equation and determine the temperature distribution through the sphere's wall. The results corresponds with the results from finite element method.
- The distributions of stress and elastic deformation derived from the analytical method are in good agreement with the finite element results.
- While the material gradient constant has a significant influence on the distribution of elastic stress and strain, it does not affect the steady-state creep stress.
- Due to the increase of creeping strains over time, stresses are rearranged to a new distribution. Afterward, stress components almost remain unchanged, while creep strain rises continuously. The rearrangement time depends on the FGM constants.
- The inner surface of the FGM vessel experiences the greatest radial and circumferential strain rates.
- By progressing creep strains, tensile stress moves from the high-stress points to the points with lower strain rates.
- Employing higher order of the Taylor series produces more accurate creep strain and stress. In the cases of thinner-wall spheres or FGM with lower constants, lower orders of the series can be employed.

Declaration of conflicting interests

The authors declare that there is no conflict of interest.

References

[1] H.-S. Shen, Functionally graded materials: Nonlinear analysis of plates and shells, ed., CRC Press, 2016,

[2] A. Amiri Delouei, A. Emamian, S. Karimnejad, H. Sajjadi, A. Tarokh, "On 2d asymmetric heat conduction in functionally graded cylindrical segments: A general exact solution", Int. J. Heat Mass Transfer, Vol. 143, No. 2019, pp. 118515.

[3] A.H. Sofiyev, N. Kuruoğlu, "The stability of fgm truncated conical shells under combined axial and

external mechanical loads in the framework of the shear deformation theory", Compos. B. Eng., Vol. 92, No. 2016, pp. 463-476.
[4] M. Niino, "Functionally gradient materials as thermal barrier for space plane", J. Jpn. Compos Mater., Vol. 13, No. 1987, pp. 257-264.
[5] N. Oxman, "Structuring materiality: Design fabrication of heterogeneous materials", Arch. Design, Vol. 80, No. 4, 2010, pp. 78-85.
[6] S.H. Mathes, H. Ruffner, U. Graf-Hausner, "The use of skin models in drug development", Adv. Drug Deliv. Rev., Vol. 69, No. 2014, pp. 81-102.
[7] G. Udupa, S.S. Rao, K. Gangadharan, "Functionally graded composite materials: An overview", Procedia Mater. Sci., Vol. 5, No. 2014, pp. 1291-1299.
[8] F.V. Tahami, A.H. Daei-Sorkhabi, F.R. Biglari, "Creep constitutive equations for cold-drawn 304l stainless steel", Mater. Sci. Eng.: A , Vol. 527, No. 18, 2010, pp. 4993-4999.
[9] J.T. Boyle, J. Spence, Stress analysis for creep, ed., Elsevier, 2013,
[10] V. Daghigh, H. Daghigh, A. Loghman, A. Simoneau, "Time-dependent creep analysis of rotating ferritic steel disk using taylor series and prandtl–reuss relation", Int. J. Mech. Sci., Vol. 77, No. 2013, pp. 40-46.
[11] Q. Cen, D.K.L. Tsang, Y. Lu, "Creep damage analysis of thin-walled pressure vessel based on continuum damage model under static loading", Int. J. Press. Vessel. Pip., Vol. 177, No. 2019, pp. 103994.
[12] D. Pathania, G. Verma, "Temperature and pressure dependent creep stress analysis of spherical shell", Int. J. Appl. Mech. Eng., Vol. 24, No. 1, 2019, pp. 105-115.
[13] M. Eslami, M. Babaei, R. Poultangari, "Thermal and mechanical stresses in a functionally graded thick sphere", Int. J. Press. Vessel. Pip., Vol. 82, No. 7, 2005, pp. 522-527.
[14] Y. Bayat, M. Ghannad, H. Torabi, "Analytical and numerical analysis for the fgm thick sphere under combined pressure and temperature loading", Arch. Appl. Mech., Vol. 82, No. 2, 2012, pp. 229-242.
[15] E.-S. Habib, M.A. El-Hadek, A. El-Megharbel, "Stress analysis for cylinder made of fgm and subjected to thermo-mechanical loadings", J. Met., Vol. 9, No. 1, 2019, pp. 4.
[16] A. Loghman, A. Ghorbanpour Arani, S.M.A. Aleayoub, "Time-dependent creep stress redistribution analysis of thick-walled functionally graded spheres", Mech. Time Depend. Mater., Vol. 15, No. 4, 2011, pp. 353-365.
[17] J. Jafari Fesharaki, A. Loghman, M. Yazdipoor, S. Golabi, "Semi-analytical solution of time-dependent thermomechanical creep behavior of fgm hollow spheres", Mech. Time Depend. Mater., Vol. 18, No. 1, 2014, pp. 41-53.
[18] Y.Y. Yang, "Time-dependent stress analysis in functionally graded materials", Int. J. Solids Struct., Vol. 37, No. 51, 2000, pp. 7593-7608.
[19] K. Daneshjou, M. Bakhtiari, R. Alibakhshi, M. Fakoor, "Transient thermal analysis in 2d orthotropic fg hollow cylinder with heat source", Int. J. Heat Mass Transfer, Vol. 89, No. 2015, pp. 977-984.
[20] A. Amiri Delouei, A. Emamian, S. Karimnejad, H. Sajjadi, D. Jing, "Two-dimensional analytical solution for temperature distribution in fg hollow spheres: General thermal boundary conditions", INT. COMMUN. HEAT MASS, Vol. 113, No. 2020, pp. 104531.
[21] M.Z. Nejad, M.D. Kashkoli, "Time-dependent thermo-creep analysis of rotating fgm thick-walled cylindrical pressure vessels under heat flux", Int. J. Eng. Sci., Vol. 82, No. 2014, pp. 222-237.
[22] S.R. Holdsworth, M. Askins, A. Baker, E. Gariboldi, S. Holmström, A. Klenk, M. Ringel, G. Merckling, R. Sandstrom, M. Schwienheer, S. Spigarelli, "Factors influencing creep model equation selection", Int. J. Press. Vessel. Pip., Vol. 85, No. 1, 2008, pp. 80-88.
[23] V. Kobelev, "Some basic solutions for nonlinear creep", Int. J. Solids Struct., Vol. 51, No. 19, 2014, pp. 3372-3381.